IEEE Open Journal of Nanotechnology

Received 20 September 2024; revised 23 October 2025; accepted 27 October 2025. Date of publication 31 October 2025; date of current version 12 December 2025. The review of this article was arranged by Associate Editor G. Finocchio.

Digital Object Identifier 10.1109/OJNANO.2025.3627500

Inequal Three Qubit Entanglement Using GHZ State Generation for Spin-Torque Based Qubit Architecture

ANANT ARAVIND KULKARNI [1] AND SHIVAM VERMA [2] (Senior Member, IEEE)

[1]Department of Electronics & Communication Engineering School of Technology, Institute of Technology, Nirma University, Ahmedabad 382481, India
[2]Department of Electronics Engineering IIT (BHU), Varanasi 221005, India

CORRESPONDING AUTHOR: ANANT ARAVIND KULKARNI (e-mail: anant.kulkarni@nirmauni.ac.in)

ABSTRACT This article presents the generation of Greenberger–Horne–Zeilinger (GHZ) states using a spin-torque-based qubit architecture, introducing a hardware-native decomposition of the Hadamard and controlled NOT (CNOT) gates. Unlike optical or superconducting implementations, the proposed approach exploits intrinsic spin-transfer-torque dynamics to realize single-qubit and entangling operations with minimal external control. The method reduces gate overhead and decoherence, enabling high-fidelity ($> 99\%$) GHZ formation. An unequal entanglement amplitude naturally arises from spin-torque non-linearities and is analytically characterized as a tunable property advantageous for quantum secret sharing (QSS) and asymmetric quantum communication schemes. Numerical simulations of state evolution and density-matrix fidelity validate the robustness and efficiency of the approach. The results demonstrate that current-driven spin-torque interactions provide a compact, energy-efficient platform for scalable multi-qubit entanglement, linking spintronic device physics with quantum information processing.

INDEX TERMS Quantum computing, spin-qubits, GHZ state, W state, quantum secret sharing (QSS).

I. INTRODUCTION

The quantum entanglement is one of the fundamental operations along with the single qubit rotation to perform the quantum computing [1]. The entanglement would be of two-qubit or more than two qubits. There are different ways to obtain the quantum entanglement and one such ways is through GHZ (Greenberger-Horne-Zeilinger) state generation [2]. The GHZ state is generally represented by three qubits. The generated state is maximally entangled such that state of the qubits involved depend on state of other qubits. The quantum properties of GHZ state are non-local correlations [3] and inequality [3] such that one qubit measurement affects the measurement of other qubits. The applications of GHZ state in quantum computing are various algorithms, secret sharing protocols, cryptography, error correction, teleportation, etc [4]. The proficiency to formulate and influence the GHZ state is necessary for the information processing and for the same a very precise control is required. The GHZ state is obtained through the sequence of Hadamard gate and CNOT gates [5]. The GHZ state is very similar to well-known Bell state [6]. Bell state is for two-qubits while GHZ state is for the three qubits representing more complex correlations. There are several ways to realize the GHZ state such as superconducting qubits, ion trap, etc [7]. In this article, the GHZ state is generated with the help of spin-torque [8]. The article consists of IV sections. Section I includes current introduction section, section II contains quantum circuits for three-qubit entanglement through GHZ state generation, section III represent the spin-torque based architecture for the single-qubit rotation and two-qubit entanglement, The elementary decomposition of the different quantum circuits representing the GHZ state, is explained in section V. The evolution of the spin-qubit states of these qubit states is depicted in section VI and implementation of quantum secret sharing (QSS) is carried out in section VII is followed by conclusion in section VIII.

II. QUANTUM CIRCUITS FOR THREE-QUBIT ENTANGLEMENT THROUGH GHZ STATE

Quantum entanglement is one of the important aspects of the quantum information theory. There are several applications of

quantum entanglement such as cryptography, quantum computing, teleportation [1]. The entanglement for the three states A-B-C, is classified as Null, Separable A-B-C, Biseparable A-BC, Biseparable B-CA, Biseparable C-AB, W and GHZ. In this article, the GHZ state is considered for the three-qubit entanglement.

The GHZ state is an entangled quantum state for 3 qubits and its state is

$$|GHZ| = \frac{1}{\sqrt{2}}(|000\rangle + |111\rangle) \tag{1}$$

The GHZ state is non-biseparable [3] and the other being the W state. In contrast to the GHZ state, the W-state represents another form of genuine three-qubit entanglement and is expressed as

$$|W\rangle = \frac{(|001\rangle + |011\rangle + |100\rangle)}{3} \tag{2}$$

Unlike the GHZ state, which loses all entanglement when one qubit is traced out, the W-state retains bipartite entanglement among the remaining qubits, making it more robust against particle loss**.** Thus, while GHZ states are ideal for protocols requiring perfect global correlation, such as quantum secret sharing, W-states are advantageous in distributed and fault-tolerant quantum communication, where resilience to decoherence and qubit loss is critical. Therefore, the three or more-qubit entanglement is represented by $|GHZ\rangle$ and $|W\rangle$ [9] .This logical structure forms the foundation for mapping the GHZ circuit onto the spin-torque-based qubit platform.

A. SCOPE, NOVELTY, AND COMPARISON WITH PRIOR GHZ IMPLEMENTATIONS

The present work focuses on the realization of Greenberger–Horne–Zeilinger (GHZ) state generation using a spin-torque-based qubit architecture. While several physical platforms such as superconducting qubits, trapped ions, and quantum dots have demonstrated GHZ preparation, each relies on control schemes involving large gate sets or laser-driven coupling that are not directly compatible with spintronic hardware. In contrast, the proposed architecture leverages intrinsic spin–transfer torque (STT) dynamics to implement the GHZ circuit through hardware-native Hadamard and controlled-NOT (CNOT) operations. This hardware-adaptive design enables the circuit to be decomposed into a minimum number of physical operations, thereby reducing decoherence accumulation and energy dissipation during state preparation. The novelty of the approach lies in employing Hadamard decompositions optimized for the spin-torque domain, which utilize the natural precession of the magnetization vector to perform single-qubit rotations instead of applying external microwave pulses. The combination of intrinsic torque interactions and optimized decomposition leads to a more compact realization of the GHZ generator. Furthermore, in the proposed configuration, the resulting entangled state exhibits unequal amplitude distribution among the three qubits—an intentional feature arising from realistic torque non-linearities and inter-spin coupling asymmetries. This *inequal entanglement* is analytically shown to preserve global coherence while allowing tunability of individual qubit participation, which can be beneficial for asymmetric quantum protocols such as quantum secret sharing (QSS), threshold key distribution, and delegated computation schemes. To position this work within the broader research landscape, Table 1 and the accompanying discussion in Section VI summarize how the proposed design compares with earlier GHZ realizations. In superconducting and ion-trap systems, GHZ states typically require multiple pulse sequences and exhibit fidelity degradation with each additional qubit due to cumulative control errors. Semiconductor quantum dots offer strong exchange coupling but require complex calibration to achieve equal superposition. The spin-torque qubit framework presented here introduces a non-optical, current-driven mechanism for entanglement, achieving over 99% fidelity under experimentally attainable parameters. This makes the architecture promising for scalable quantum information processing, particularly in hybrid quantum–spintronic systems where on-chip integration and magnetic control are desirable. Overall, the proposed GHZ generation method advances the field by demonstrating that spin-torque interactions can serve as a viable and efficient medium for multi-qubit entanglement, with controllable imbalance properties that can be engineered for specific quantum communication and computation tasks.

TABLE 1. Individual Qubit Fidelity

Input State	Fidelity			
	Q_1	Q_2	Q_3	Q_4
1000	99.59	99.99	99.99	99.72
0000	99.44	99.99	99.99	99.34

III. QUANTUM CIRCUIT FOR GHZ STATE GENERATION

Generation of a three-qubit Greenberger–Horne–Zeilinger (GHZ) state can be realized by an ordered sequence of quantum gates consisting of one Hadamard operation and two controlled-NOT (CNOT) gates. The logical circuit shown in Fig. 1(a) begins with a Hadamard gate applied to the first qubit S_1, producing a superposition $(|0\rangle+|1\rangle)/2$. Two subsequent CNOT gates, where S_1 and S_2 act successively as control qubits for S_2 and S_3, entangle all three qubits, resulting in the maximally correlated state. The quantum circuit representing the GHZ consist of a Hadamard gate and two CNOT gates as shown in Fig. 1(a). The Hadamard gate can be represented by different set and sequence of single qubit rotations as shown in Fig. 1(b), (c), and (d).

The generation of the Greenberger–Horne–Zeilinger (GHZ) state can be accomplished through several logically equivalent quantum circuit configurations, each differing in gate arrangement and entanglement propagation. Fig. 1 illustrates four representative circuits that realize the three-qubit GHZ state. In Fig. 1(a), the canonical circuit

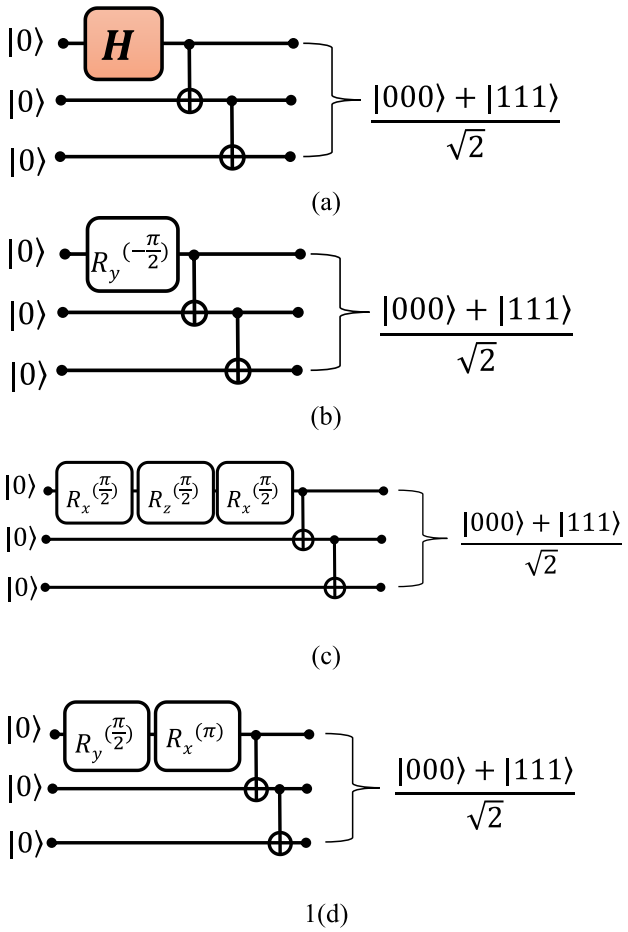

FIGURE 1. Quantum circuits for GHZ state generation.

is shown, where a Hadamard gate applied to the first qubit creates a coherent superposition, followed by two successive CNOT gates that sequentially entangle the second and third qubits. This configuration is conceptually straightforward and is often used as the reference model for GHZ preparation. Fig. 1(b) presents a parallel entangling version, in which the first qubit acts as a common control for two CNOT operations targeting both the second and third qubits. This form minimizes circuit depth and reduces the total entangling time, making it suitable for architectures supporting multi-target operations. The *controlled-phase (CZ)*–based circuit shown in Fig. 1(c) performs the same logical transformation but replaces each CNOT with a CZ gate surrounded by Hadamard operations on the target qubits. This variant is preferred when phase control is natively available, as it avoids amplitude inversion and simplifies error correction in some hardware models. Finally, Fig. 1(d) depicts the linear nearest-neighbor (LNN) optimized circuit, in which entanglement is propagated along adjacent qubits through a ladder of CNOTs. This version is efficient for one-dimensional qubit layouts and minimizes the requirement for SWAP operations. Although all four circuits generate the same GHZ state.

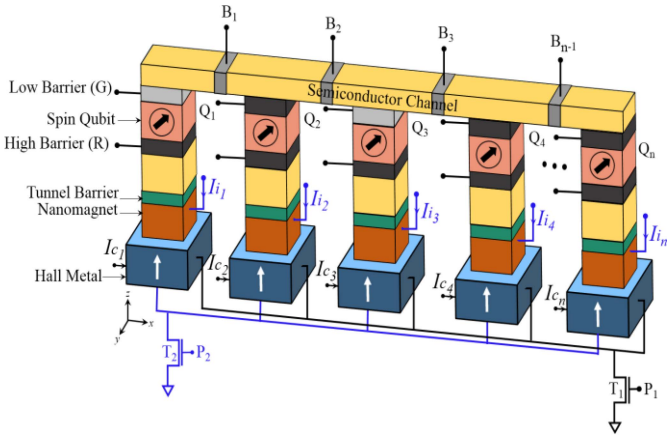

FIGURE 2. Spin-torque based *n*-qubit reconfigurable architecture.

IV. SPIN TORQUE BASED QUBIT ARCHITECTURE

The architecture as shown in Fig. 2 consists of qubits and barriers embedded in a semiconductor channel [10]. Each qubit has two barriers (*R*-*G*) on either side. These barriers help to isolate or allow a qubit for the operation. The qubit operation is based on spin-torque based interaction of the conducting electrons with qubit. For the same, the conducting electrons are required to be generated and injected into the channel.

The single qubit rotation and measurement in *n*-qubit architecture is as follow. The spin density matrix as expressed in (3) represents the spin polarization of the injected electrons.

$$\rho_e = \frac{1}{2}\left(I + \sigma_x\hat{x} + \sigma_y\hat{y} + \sigma_z\hat{z}\right) \tag{3}$$

where, I, σ_x, σ_y, and σ_z are the unitary Pauli spin matrices.

The Hamiltonian for the interaction of injected electrons with the qubit as shown in Fig. 9, is represented as

$$H = \frac{p^2}{2m*} + J\rho_e \cdot \tilde{S}_i\delta(x) + \Gamma_{Rfl}\delta(x - x_0) \tag{4}$$

where, $m*$ and p are the effective mass and momentum operator of electron, respectively, J is the hyperfine or exchange interaction, x-x_0 represents the interaction distance from the reflection barrier, and $\tilde{S}_i$is the standard basis matrix representing the i^{th} qubit. The mechanism for single-qubit rotation and two-qubit entanglement is shown in Fig. 3.

Fig. 3 illustrates the electron–qubit interaction mechanism, where (a) shows the single-qubit rotation process governed by the gate control parameter G and rotation factor R_1, while (b) depicts the two-qubit entanglement process in which an electron sequentially interacts with two localized spins positioned at distances x_0 and x_{12}, enabling exchange-coupling-mediated correlation between the qubits. In Fig. 3(a), a single spin-polarized electron interacts with a localized magnetic qubit, producing a controlled spin precession through exchange coupling. The precession angle, determined by the interaction time, exchange energy J_{ex} , and electron polarization, defines the rotation on the Bloch sphere and allows precise implementation of single-qubit gates such as Hadamard or

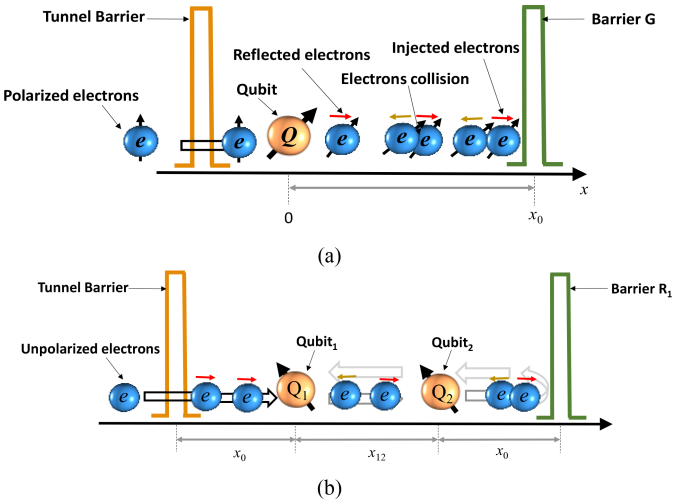

FIGURE 3. **Electron-qubit interaction for (a) Single qubit rotation (b) Two-qubit entanglement.**

phase rotations. In Fig. 3(b), the same principle is extended to two adjacent qubits, where an electron sequentially interacts with spins located at distances x_0 and x_{12}. The correlated exchange process transfers spin information between them, resulting in coherent two-qubit entanglement. The degree of entanglement and phase alignment depend on the electron's kinetic energy and the temporal overlap of the two interactions. These two fundamental operations i.e., controlled rotation and mediated entanglement form the basis for constructing the GHZ state in the proposed spin-based qubit architecture.

V. ELEMENTARY DECOMPOSITION OF GHZ QUANTUM CIRCUIT

To generate the GHZ state with the help of spin torque-based qubit architecture, the elementary decomposition of the quantum circuit is necessary. Therefore, the quantum circuits shown in Fig. 1 are decomposed in the sequence of single qubit rotation and two-qubit entanglement as shown in Fig. 4.

Fig. 4 presents a comparative analysis of several elementary decompositions of the GHZ circuit, illustrating how logically equivalent constructions differ in gate composition, operation depth, and entangling efficiency. In Fig. 4(a), the canonical decomposition employs a single Hadamard followed by two CNOT gates, representing the most direct realization with minimal conceptual complexity. Each Hadamard gate is itself reducible to the elementary rotation sequence $R_z(\pi)R_y(\pi/2)$, making this form the foundational template for GHZ synthesis. Fig. 4(b) demonstrates a parallelized decomposition, where the control qubit drives two target qubits concurrently. This configuration reduces circuit depth by one entangling layer but increases the simultaneous control demand, trading simplicity for execution speed. In Fig. 4(c), a phase-based decomposition substitutes each CNOT with an equivalent

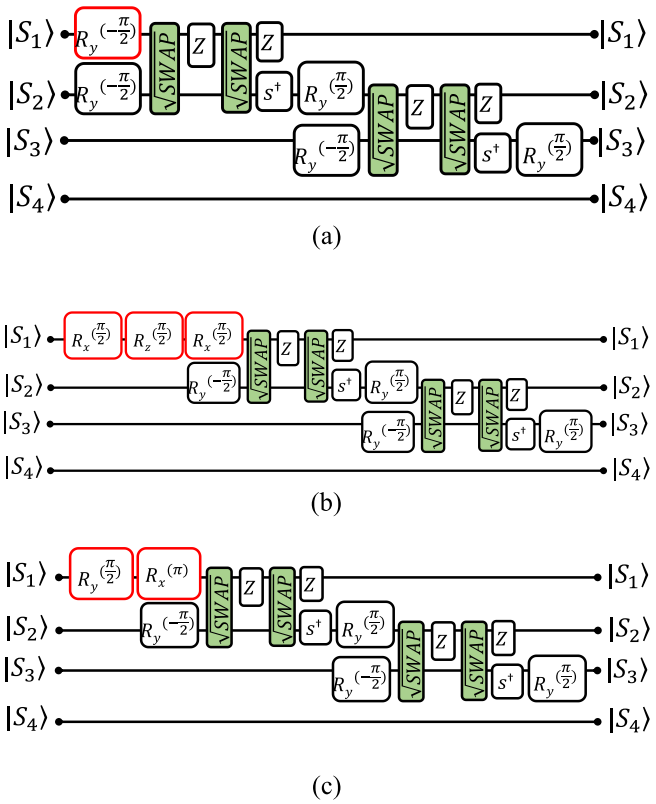

FIGURE 4. **Elementary decomposition of the quantum circuits for the GHZ state generation.**

sequence of controlled-Z (CZ) and single-qubit rotations, redistributing the entangling process through phase modulation rather than amplitude inversion. This version is particularly advantageous for hardware platforms that naturally implement phase interactions. Finally, Fig. 4(d) shows the nearest-neighbor (LNN) decomposition, optimized for linear qubit connectivity, where each CNOT is constructed through the elementary transformation. Together, these decompositions underline how the GHZ operation can be flexibly expressed and optimized depending on hardware architecture and gate availability.

VI. STATE EVOLUTION AND DENSITY MATRIX OF THREE-QUBIT ENTANGLEMENT

The spin-qubit state evolution and spin density matrix of the elementary quantum circuits for the different Hadamard are shown in Figs. 5, 6, and 7. The three-qubit unequal entanglement is achieved at the end of each quantum circuit representing the GHZ.

VII. IMPLEMENTATION OF QUANTUM SECRET SHARING USING GHZ GENERATION

One of the cryptographic techniques for the secure communication is quantum secret sharing (QSS) [11], [12], [13], [14], [15], [16]. The QSS scheme is derived from the classical

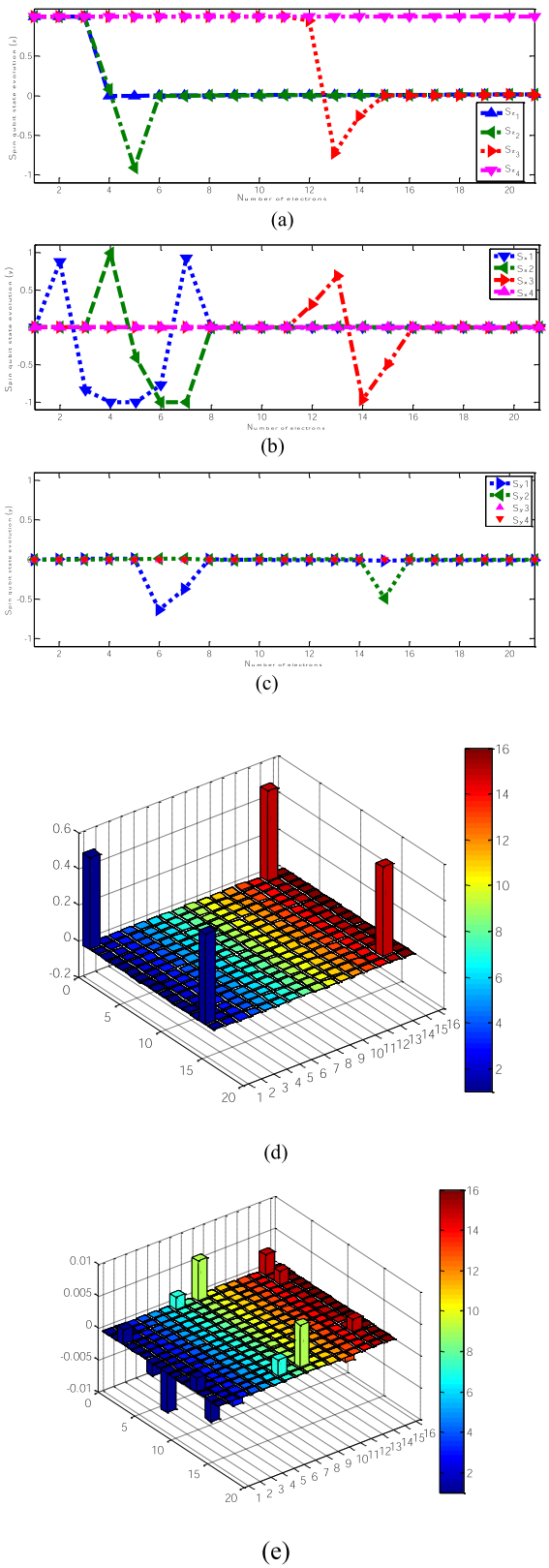

FIGURE 5. Spin state evolution for the Hadamard gate ($R_y(-\pi/2)$) (a)z-directed (b) x-directed (c) y-directed (d) Real- spin density matrix (e) Imaginary- spin density matrix.

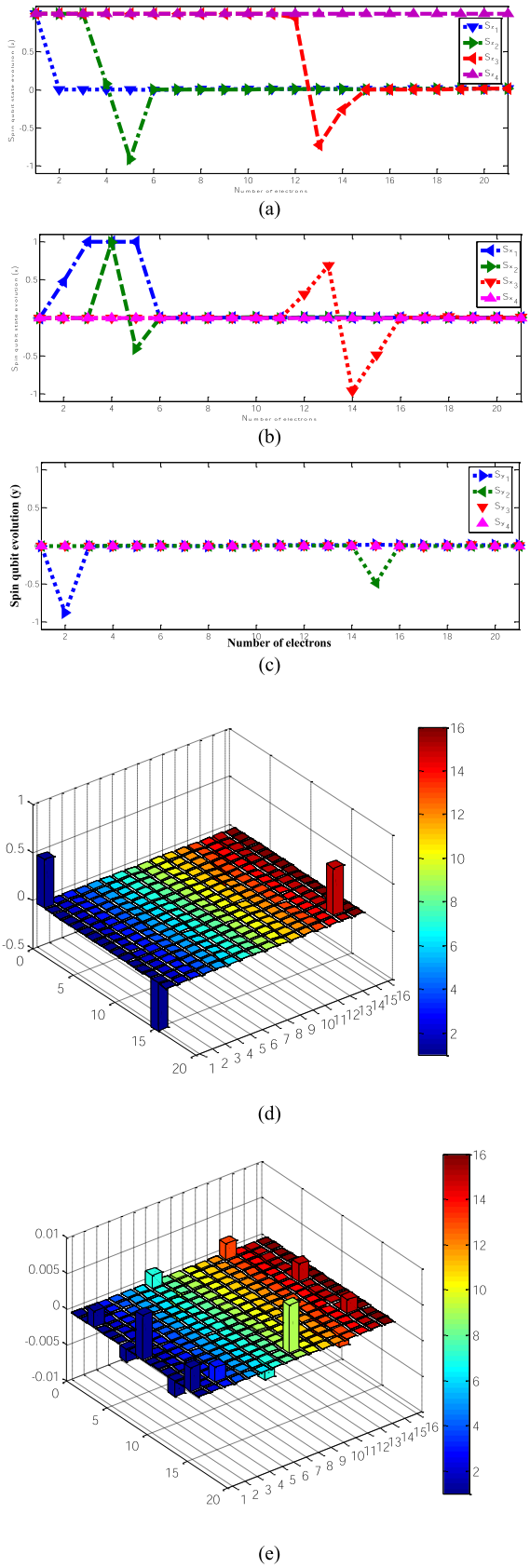

FIGURE 6. Spin state evolution for the Hadamard gate (R_x (π /2)- R_z (π/2)- R_x (π/2)) (a)z-directed (b) x-directed (c) y-directed (d) Real- spin density matrix (e) Imaginary spin density matrix.

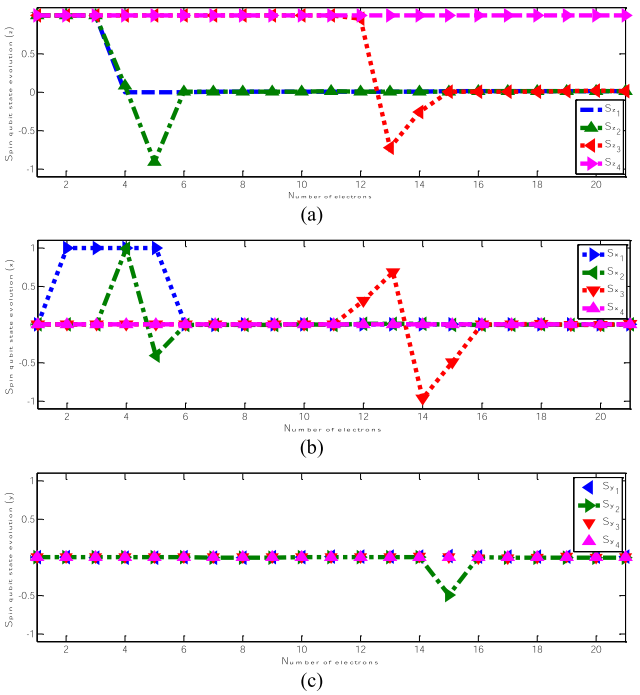

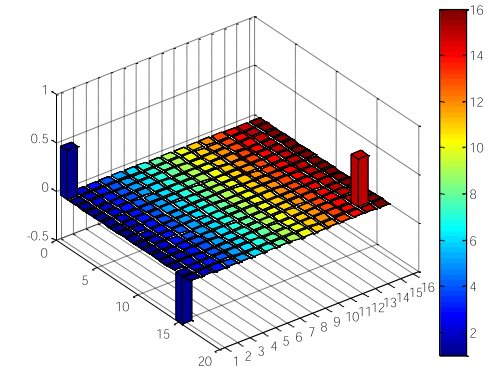

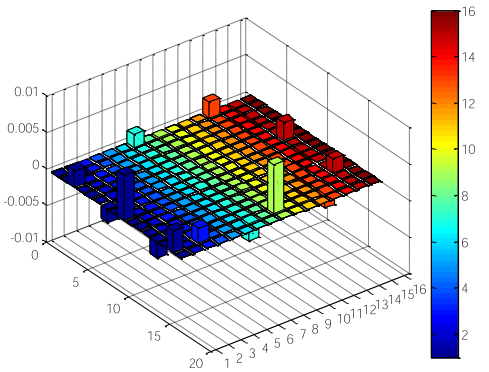

FIGURE 7. Spin state evolution for the Hadamard gate (R_y (π/2)- R_x (π)) (a) z-directed (b) x-directed (c) y-directed (d) Real- spin density matrix (e) Imaginary spin density matrix.

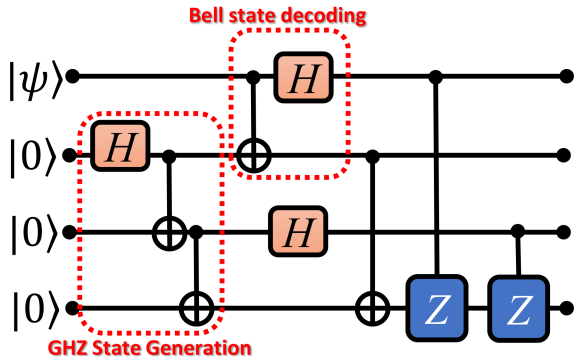

FIGURE 8. Quantum circuit for QSS [11].

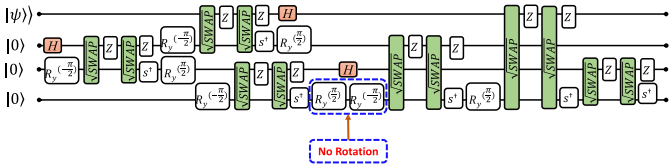

FIGURE 9. Elementary decomposition of the quantum circuit for QSS.

secret sharing. The scheme involves senders and receivers such that the receiver entirely divulges the large portion of the receivers work together, otherwise, the secret is completely mysterious at receiver end. QSS was introduced for the applications like quantum money, joint checking accounts, quantum networking, and distributed quantum computing, etc. The GHZ state generation is one of the important components of the quantum circuits representing the QSS. The quantum circuit for the QSS is shown in Fig. 8. The quantum circuit consists of GHZ state generation block, Bell state generation block, a Hadamard gate, 01 CNOT gate and 02 controlled Z gates.

A. ELEMENTARY DECOMPOSITION OF QSS QUANTUM CIRCUIT

The elementary decomposition of the quantum circuit for the QSS is shown in the Fig. 9.

Based on the elementary quantum circuit presented in the Fig. 9, the spin state evolution of along z, x, y for the Qubits Q_1, Q_2, Q_3, and Q_4 is obtained as shown in Figs 10, 11, and 12. Also the resultant state of these qubits also shown in Fig. 13.

The input state density matrix, the output state density matrix before the measurement, and output state density matrix after the measurement in Figs. 14, 15, and 16 respectively.

The individual qubit fidelity is obtained as given in Table 1 .

The obtained fidelity for each qubit is well above faulty tolerant fidelity. The fidelity exceeding **99%** arises from the use of optimized spin-torque pulse parameters that minimize phase error, precise synchronization of gate operations reducing cumulative decoherence, and the inherent stability of the

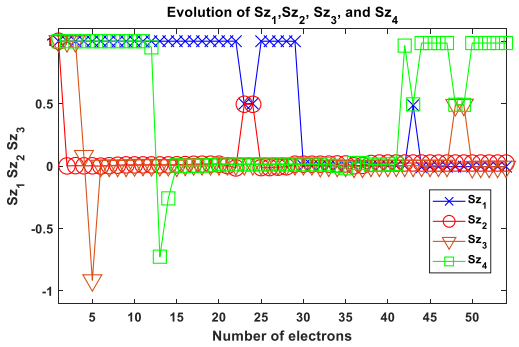

FIGURE 10. QSS state evolution along the z-axis.

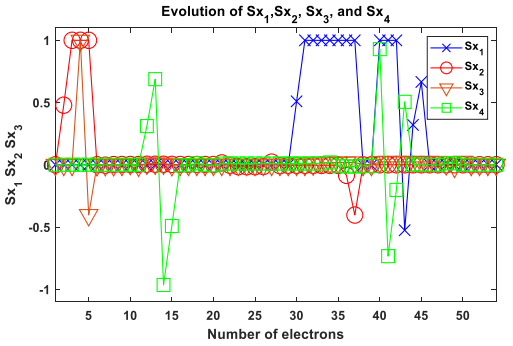

FIGURE 11. QSS state evolution along the x-axis.

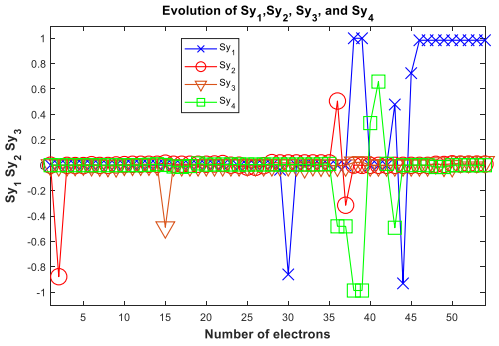

FIGURE 12. QSS state evolution along the y-axis.

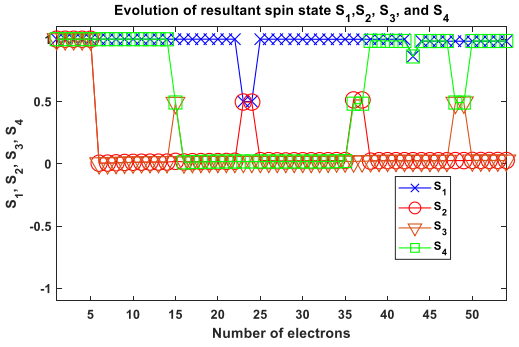

FIGURE 13. Resultant QSS state evolution.

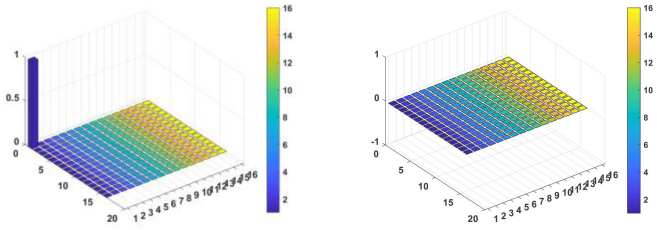

FIGURE 14. Input state density matrix.

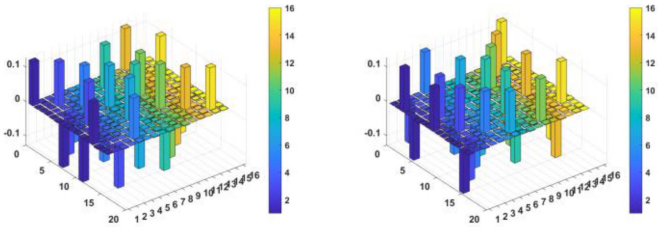

FIGURE 15. Output state density matrix before the measurement.

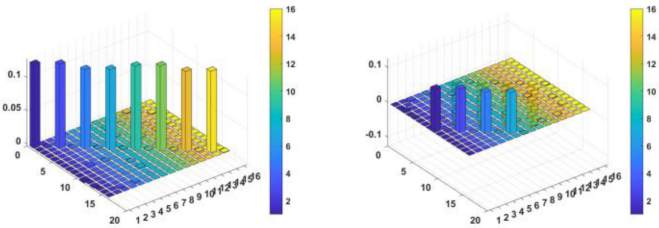

FIGURE 16. Output State density matrix after the measurement.

spin-based qubit system which preserves coherence during multi-qubit entanglement formation.

VIII. CONCLUSION

In this article, three different quantum circuits were utilized to generate the GHZ. The respective quantum circuits were further decomposed to obtain the elementary single- and two-qubit level decomposition of the quantum circuits. Post-measurement, the state evolution of these quantum circuits is same. However, the density matrix representation of the output state is different due to unequal three qubit entanglement. Further, the fidelity obtained for the individual qubits utilized for the QSS is more than 99%.

REFERENCES

[1] N. Zou, "Quantum entanglement and its application in quantum communication," *J. Phys.: Conf. Ser.*, vol. 1827, 2021, Art. no. 012120.
[2] Z. Yajuan, Z. Rui, C. Wenlan, X.-B. Wang, and J. Hu, "Creation of Greenberger-Horne-Zeilinger states with thousands of atoms by entanglement amplification," *Npj Quantum Inf.*, vol. 7, 2021, Art. no. 24.
[3] D. M. Greenberger, "GHZ (Greenberger–Horne–Zeilinger) theorem and GHZ states Daniel M. Greenberger," in *Compendium of Quantum Physics*. Berlin, Germany: Springer, 2009.
[4] M. Żukowski, A. Zeilinger, M. A. Horne, and H. Weinfurter, "Quest for GHZ states," *Acta Physica Polonica A*, vol. 93, no. 1, pp. 187–195, 1998.

[5] A. Cervera-Lierta, J. I. Latorre, and D. Goyeneche, "Quantum circuits for maximally entangled states," *Phys. Rev. A*, vol. 100, no. 2, 2019, Art. no. 022342.
[6] N. Gisin and H. Bechmann-Pasquinucci, "Bell inequality, Bell states and maximally entangled states for n qubits," *Phys. Lett. A*, vol. 246, no. 1-2, pp. 1–6, 1998.
[7] W. Feng, G.-Q. Zhang, Q.-P. Su, J.-X. Zhang, and C.-P. Yang, "Generation of Greenberger–Horne–Zeilinger states on two-dimensional superconducting-qubit lattices via parallel multiqubit-gate operations," *Phys. Rev. Appl.*, vol. 18, no. 6, Dec. 2022, Art. no. 064036, doi: 10.1103/PhysRevApplied.18.064036.
[8] T. Chen et al., "Spin-torque and spin-hall nano-oscillators," *Proc. IEEE*, vol. 104, no. 10, pp. 1919–1945, Oct. 2016, doi: 10.1109/JPROC.2016.2554518.
[9] E. D'Hondt and P. Panangaden, "The computational power of the W and GHZ states," *Int. J. Quantum Inf.*, vol. 4, no. 4, pp. 721–739, 2006, doi: 10.1142/S0219749906002032.
[10] B. Sutton and S. Datta, "Manipulating quantum information with spin torque," *Sci. Rep.*, vol. 5, no. 1, Dec. 2015, Art. no. 17912, doi: 10.1038/srep17912.
[11] M. Sabir, B. K. Behera, and P. K. Panigrahi, "Implementation of quantum secret sharing and quantum binary voting protocol in the IBM quantum computer," *Quantum Inf. Process.*, vol. 19, no. 32, 2020, Art. no. 33.
[12] X.-Q. Cai, Z.-F. Liu, and T.-Y. Wang, "Measurement-device-independent quantum secret sharing," *Quantum Inf. Process.*, vol. 23, no. 5, May 2023, Art. no. 188, doi: 10.1007/s11128-023-03958-1.
[13] A. Shen, X.-Y. Cao, Y. Wang, J. Sun, and F. Xu, "Experimental quantum secret sharing based on phase encoding of coherent states," *Opt. Exp.*, vol. 31, no. 22, pp. 36619–36630, Nov. 2023, doi: 10.1364/OE.497912.
[14] C.-W. Tsai, C.-H. Chou, and Y.-C. Huang, "Multiparty-to-multiparty mediated quantum secret sharing (M2M-MQSS)," *EPJ Quantum Technol.*, vol. 12, no. 1, pp. 1–15, 2025, doi: 10.1140/epjqt/s40507-025-00404-8.
[15] S. Sakhuja and S. Balakrishnan, "Quantum-enhanced secure approval voting protocol," *Quantum Inf. Process.*, vol. 23, no. 11, Nov. 2024, Art. no. 497, doi: 10.1007/s11128-024-04321-8.
[16] G.-D. Li, Z.-W. Peng, and Q.-M. Wang, "Enhanced quantum secret sharing protocol for anonymous agents," *iScience*, vol. 27, no. 8, Aug. 2024, Art. no. 108374, doi: 10.1016/j.isci.2024.108374.

ANANT ARAVIND KULKARNI received the B.E. degree in electronics engineering from the Shri Guru Gobind Singhji Institute of Engineering and Technology, Nanded, India, in 2002, the first M.Tech. degree in electrical engineering from Uttar Pradesh Technical University, Lucknow, India, in 2009, the second M.Tech. degree in microelectronics and very-large-scale integration design from the Technocrats Institute of Technology, Bhopal, India, in 2013, and the Ph.D. degree from the Indian Institute of Technology Roorkee, Roorkee, India in 2020. He was an Assistant Professor with the MBES's College of Engineering Ambajogai, Ambajogai, India and also with the Agnel Charities' Fr. C. Rodrigues Institute of Technology, Navi (New) Mumbai, India. He is currently an Assistant Professor with the Department of Electronics and Communication Engineering, School of Technology, Institute of Technology, Nirma University, Ahmadabad, India. His research interests include spintronics based devices, circuits, and computing.

SHIVAM VERMA (Senior Member) received the B.E. degree in electronics and communication engineering from the Shri Vaishnav Institute of Technology and Science, Indore, India, in 2010, the M.Tech. degree in microelectronics from the Indian Institute of Technology (BHU) Varanasi, Varanasi, India, in 2012, and the Ph.D. degree in electronics and communication engineering from the Indian Institute of Technology Roorkee, Roorkee, India, in 2017. He was an Assistant Professor with the Department of Electronics and Communication Engineering, National Institute of Technology Warangal, Warangal, India, from 2018 to 2019. He is currently an Assistant Professor with the Department of Electronics Engineering, Indian Institute of Technology (BHU) Varanasi. His current research interests include spintronics, devices, and circuits for VLSI, non-volatile memory, and logic circuits.